Nanocoatings for healing surface defects of glass fibres and improving interfacial adhesion

Oberflächendefekte an Glas und anderen spröden Materialien bewirken signifikant niedrigere mechanische Eigenschaften als deren theoretische Werte. Beschichtungen können genutzt werden, um die Oberflächendefekte „auszuheilen“ und die Oberflächeneigenschaften zu modifizieren. Wir beschreiben hier einen online Prozess, mit dem nanoskalige Hybridcoatings auf Basis von Styren-Butadien-Copolymeren mit Single- oder Multi-wall-Carbon-Nanotubes (SWCNTs, MWCNTs) und/oder Nanoclay zur Verbesserung der mechanischen Eigenschaften und als Barriereschicht auf alkaliresistenten (ARG) und E-Glasfilamenten angewandt werden. Unsere Ergebnisse zeigen sowohl signifikant verbesserte mechanische Eigenschaften als auch Korrosions-beständigkeit durch die Nanostrukturierung und Funktionalisierung der traditionellen Glasfasern. Mit einem geringen Gehalt an Nanotubes (0,2 Ma.-% in der Schlichte) steigt die Zugfestigkeit der „geheilten“ Glasfaser um bis zu 70 %. Für mit Nanoclay beschichtete Fasern kann nach einer aggressiven Alkali-behandlung keine Festigkeitsvariation nachgewiesen werden. Wir führen einen Effektivitätsfaktor der Ausheilung ein und schlussfolgern, dass der Elastizitätsmodul der Beschichtung, die Schichtdicke und die Rauheit für die Verbesserung der mechanischen Eigenschaften verantwortlich sind. Neben der verbesserten Faserfestigkeit und Korrosionsbeständigkeit sind die Grenzflächenparameter erhöht.

Keywords
glass fibres
surface defects healing
nanocomposite
coating
interfacial adhesion

Bearbeiter
S.L. Gao
E. Mäder
R. Plonka
C. Scheffler

Förderer
Deutsche Forschungsgemeinschaft

Kooperation
Technische Universität Dresden, Institut für Baustoffe,
DFG-Sonderforschungsbereich 528 „Textile Bewehrungen zur bautechnischen Verstärkung und Instandsetzung“
DFG-Sonderforschungsbereich 639 „Textilverstärkte Verbundkomponenten für funktionsintegrierende Mischbauweisen bei komplexen Leichtbauanwendungen“

Gastwissenschaftler
Dr. S. Zhandarov,
Belorussische Akademie der Wissenschaften, Metall-Polymer-Forschungsinstitut Gomel, Weißrussland

Introduction

Surface defects of brittle materials cause actual tensile strength much lower than the ultimate theoretical strength. The nanoscale surface defects providing extra stress at the tip of the cracks can lead to stress-corrosion cracking at low stress level, particularly in a humid environment. Healing nanoscale surface flaws and enhancing materials' lifetime by nanocoatings are, therefore, important for many traditional materials. Our recent work showed that the tensile strength of alkali-resistant and E-glass fibres can be well described by bimodal Weibull cumulative distribution function for different sizing systems and improved mechanical properties and environmental durability are achieved by suited sizings [1].

Reinforcement with nanomaterials is a topic of significant current interest. It is well known that surface defect-free and high purity carbon nanotubes have exceptionally high Young's modulus and tensile strength. However, an efficient utilization of the excellent properties of nanoreinforcements to the microscopic and macroscopic level is a long standing problem. To date, the highest strength and Young's modulus reported in the literature are relatively disappointing: 1.8~3.2 GPa and ca. 40 GPa, respectively, for aligned nanotube composite bundles with very high volume loading of nanotubes (60 wt%) [2], which are a factor of ten below those of the component individual nanotubes because of poor integration and weak interfacial adhesion. Therefore, to find an appropriate dispersion for the nanoreinforcements to increase volume concentration, limited by chemical inertness and van der Waals attractions, is not sufficient for producing high-quality

composites. In contrast to this *super-materials degraded by defects* approach, here, we apply a *surface defects healed by super-materials* approach (Fig. 1), where the traditional alkali-resistant glass fibres (ARG) were coated using different nanostructured coating layers with low loading (< 1 wt%) of multi walled carbon nanotubes (MWCNT) and/or organo-clay (Nanofil 15, Süd-Chemie AG, Germany), to provide a protective layer against aqueous alkaline solution (5 wt % NaOH) at 20 °C for seven days. Atomic force microscopy (AFM), scanning electron microscopy (SEM), nanoindentation and single fibre tensile and pull-out tests were used to investigate in detail the local surface topography, mechanical and interfacial properties.

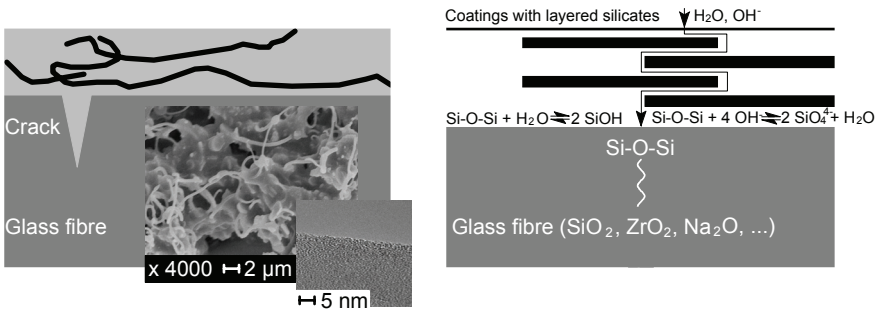

Fig. 1:
Schematics of nanostructured coatings with nanotube/layered silicate polymer network on glass fibre surface to enhance flaw healing effect and corrosion resistance. The inserts show polymer/MWCNT network by SEM and individual surface functionalized nanotube structure by transmission electron microscopy (TEM).

Results

We first examined the morphology of nanoreinforcements in coatings. Fig. 2 shows a pair of AFM topography/phase images of a nanocoating with nanotubes from identical areas captured on the glass fibre surface. Although it is normally impossible to observe the individual nanotube when it is embedded in thick coating polymer matrix, our phase image on the fibre surface where the coating layer is thin shows apparent contrast between the nanotube and polymer regions. It reveals a difference in surface or underlying material properties of the regions in terms of stiffness, viscosity and adhesion. Interestingly, the nanotubes show an irregular distribution and quite well separated from bundles which do not tend to normally agglomerate and close-packed patterns, suggesting that the high speed on-line sizing process could be utilized for separation of nanotube bundles for a wide range of composite applications.

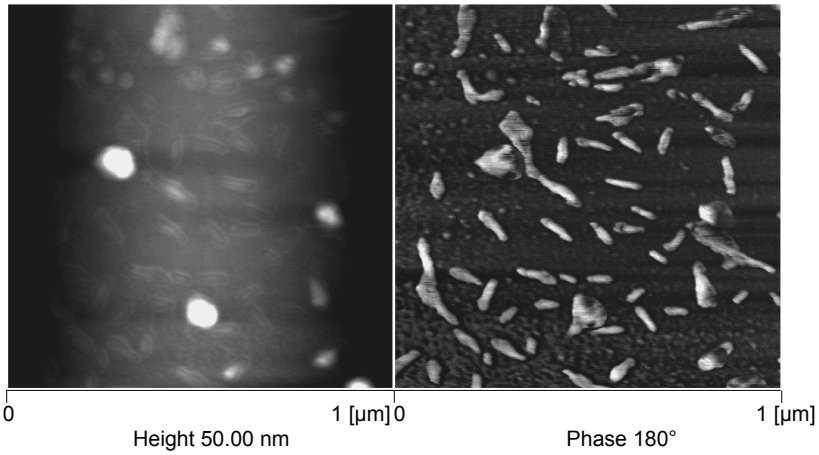

Fig. 2:
AFM topography (left) and phase (right) images of nanostructured coating with nanotubes and γ-APS/epoxy film former sizing on ARG fibre surface.

We have further examined whether the dispersed organo-clay was intercalated or exfoliated in the coatings. Individual crystallites observed by AFM topography (Fig. 3a) display the lath-type morphology of hectorite, consisting of a layered structure of aluminum sandwiched between two layers of silicon.

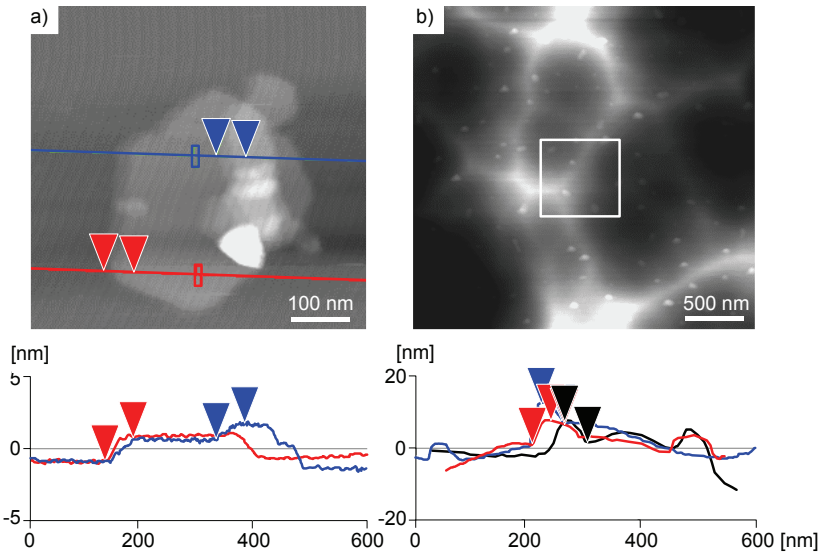

Fig. 3:
AFM topography and section analysis (bottom) of (a) layered silicate clay and (b) fracture surface of coating with clay after alkali treatment. The distance between clay sheets is ~1.5 nm shown by section profile of the individual clay sheet along the lines in the top view of the left figure.

The measured height of individual particles equals ~ 1.5 nm, which corresponds to the distance between two single smectite layers. Fig. 3b shows that the fracture surface topography of coating film with clays after alkaline treatment consists of many similar shape particles. The measured thickness and lateral size of the particles are ~ 6 nm and ~ 80 nm, respectively, suggesting that the silicate layers of clay are intercalated. These clay platelets provide high surface areas of contact with the polymer matrix. Random distribution of the particles dispersed in the coating polymer matrix is clearly visible. The particles are impermeable to molecular species and limit the diffusion of hydroxyl ions to the glass surface and the crack tip. Obviously, an appreciable level of platelet content and orientation is required to provide alkali barrier enhancement.

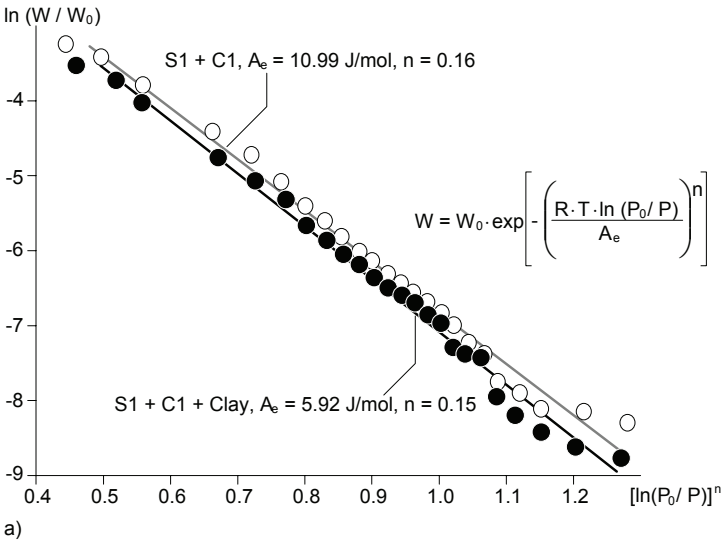

Fig. 4a:
Adsorption isotherms of water vapour on sized glass fibres fitted by the Dubinin-Astakhov equation

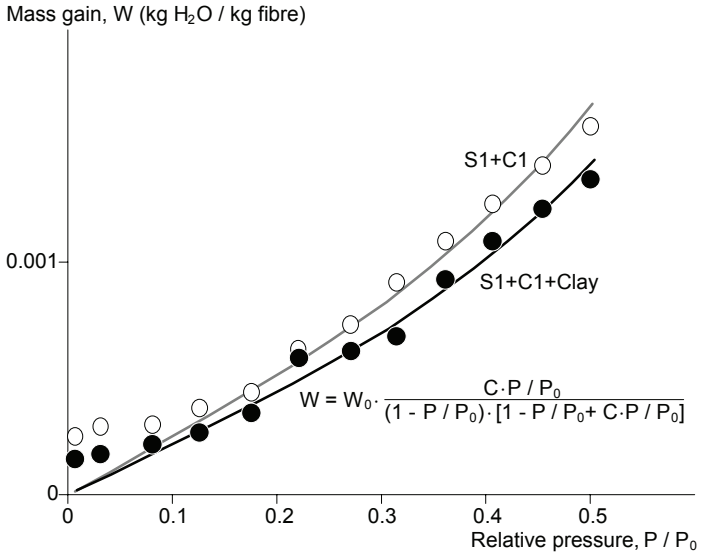

Fig. 4b:
Adsorption isotherms of water vapour on sized glass fibres fitted by the Brunnauer-Emmett-Teller equation

To understand the barrier levels that can be achieved with the nanometre-thin sheet-like layers of clay fillers in the coating, the sorption isotherms of fibres are measured. The nanoclay containing the coating has lower values of both adsorption and desorption than coating without clay at all ranges of relative pressure, particularly at high relative pressure, suggesting clay coating adsorbed less water. The adsorption isotherm was analysized by means of the Dubinin-Astakhov (DA) [3] and the Brunauer-Emmet-Teller (BET) [4] methods (see Fig. 4). The DA parameters qualitatively reflect the degree of heterogeneity (micropore volume and surface chemistry) of the materials. We found a significant decrease of the characteristic energy of adsorption for coating with nanoclay. The increased pore volume can be attributed to the large interface area between clay-clay and clay-polymer. The BET equation is based on adsorption on free surface without capillary condensation and therefore is applicable to adsorption for the mono and multilayer regions of the isotherm. The sample with nanoclay showed that water is stronger bound to the coating which is associated with the clay platelets and the interfaces adsorbing and retaining water molecules. Thus, the diffusion through the clay loaded coating would appear much slower. In addition, the maximum concentrations of bound monolayer water in the coating suggest that the moisture solvent uptake and concentration decreases accordingly when the organo-clay is dispersed in coating polymer. Since a transport barrier layer affects both diffusion and sorption, a proposed mechanism of the improved alkali-resistance is that the clay particles retain water molecules and reduce the moisture adsorption and concentration in the coating layer and coating/fibre interface. The clay particles also act as obstacles forcing both outside solution molecules and inside dissolved alkali ions diffusing to long detours round the platelets (cf. Fig. 1). A number of experimental and theoretical studies of polymer film with clay have also shown that intrinsic permeability decreases significantly, i.e., the water diffusivity was reduced to half of its value in the neat polymer. Additionally, taking into consideration chemical effects of coating, as revealed by zeta-potential measurements in our early work [5], the acidic groups (i.e. COOH) of coating polymer were dominating on fibre surface before and after NaOH treatment. Since the congruent dissolution of glass corrosion process is only valid in high pH environment, the coating with acidic character, as an alkali-deficient layer, can slow down the deterioration process by limiting the increase of the localized pH value and growth of silica gel layer.

Therefore, the clay reinforced coating layer is rather alkali-resistant because of these different physico-chemical mechanisms.

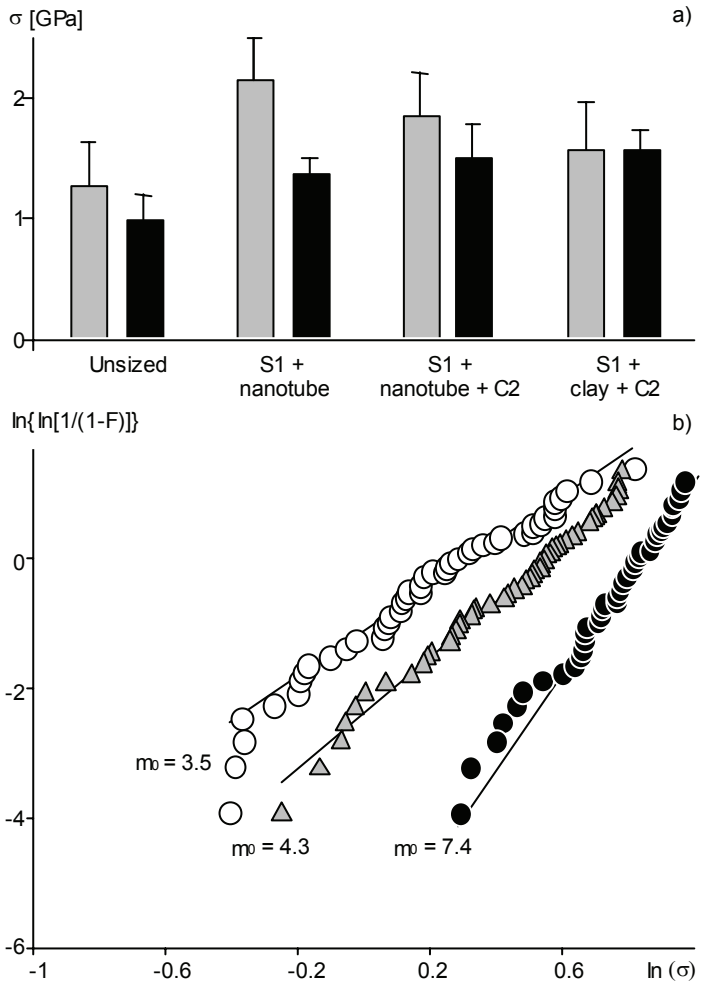

Fig. 5:
a) Effect of the nanostructured coatings with low fraction of nanoreinforcements on the ensile strength σ of ARG before (□) and after alkaline treatment in 5 wt% NaOH aqueous solution (■) for seven days in an ambient environment
b) Weibull plots of fibre fracture probability

We next investigated the tensile performance of the single fibres. Fig. 5a shows that the tensile strength of surface nanostructured ARG with both nanotubes and organo-clay is significantly improved. The fibre strength increased up to 70 % and 25 % for sized fibre with 1 wt% loading of MWCNTs or organo-clay in the sizing or coating, respectively. Because the critical flaws which limit the strength of fibres are located at the surface, the fibre fracture behaviour is strongly affected by the variation of coating properties. Interestingly, as shown in Fig. 5b, both the Weibull plot lines and Weibull modulus, m_o, of coated systems shift to higher values than those of the control. This indicates that the strength-controlling surface defects have lower heterogeneity distribution and the size of defects is reduced. In other words, the healed flaws on the coated fibres show similar flaw size, severity and homogeneity relative to those on the control fibres. The effects of alkaline attacks on the average fibre strength are also compared in Fig. 5a. It is evident that samples of clay coatings would not yield a significant strength reduction upon alkali treatment. However, a significant strength reduction for systems with nanotube sizings occurred. This can be partly compensated by an additional styrene-butadiene coating with carboxylic groups, which shows an enhanced alkali-resistance as determined by the marginal strength reduction. Therefore, the durability and alkali-resistance are also improved, particularly for the fibre with organo-clay coatings.

Overall, the coated fibres have higher strength values than the control one after alkaline corrosion, reflecting the improved environmental durability for fibres with nanostructured coatings.

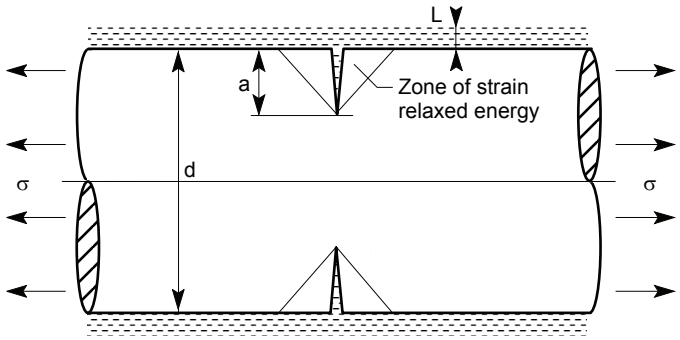

Fig. 6:
A sketch of a coated fibre with a surface flaw. The fibre is loaded in tensile stress σ and the circumferential surface flaw of length a serves as an initial crack. The fibre diameter and coating thickness are given by d and L, respectively, where a and L are much less than d.

Potential mechanisms of the mechanical property improvement include the contributions of different factors. Firstly, the coating layer and organo-silicate plates preventing moisture/alkali contact and reaction with glass lattice at a crack tip (stress corrosion). As mentioned before, the acidic groups of coating molecular interact with or absorb free cations and anions of environment leading to a slow-down of the corrosion process. Secondly, stress-redistribution and crack stopping mechanisms by coatings and nanotube's *bridging* effect as well as interface debonding/plastic deformation around crack tip take place. The mechanical 'healing' effect was regarded as a disappearance of the severe surface flaws because of an increase of the crack tip radius, the flaw filled by coatings being rather elliptical than sharp. Thirdly, compressive stress on fibre surface might prevent crack opening/propagation by the shrinkage of polymer due to solidification. To simplify the complex phenomena, we developed a simple mechanical model based on Griffith fracture mechanics to roughly estimate the strength of coated fibre [6]. A smoothly coated fibre loaded in tension having a thin circumferential crack, as shown in Fig. 6, was considered as model.

When the crack appears, the strain energy is released in a material volume adjacent to the crack. This volume comprises a conical ring whose generating lines are shown by broken lines and whose height is proportional to the crack length. On the other hand, the energy is consumed by formation of new surfaces and deformation of coatings because of an elastic constraint. According to the energy balance, the coated fibre strength, σ_f, can be expressed as

$$\sigma_f > \overline{\sigma}_f = \sqrt{\frac{2 \cdot \gamma \cdot E_f}{\left(\beta \cdot a^* - \frac{L(1+L/d) \cdot E_c}{E_f}\right)}} \qquad (1)$$

where γ is fracture surface energy and β is a constant coefficient of proportionality. E_f and E_c are Young's modulus of fibre and coatings, respectively. We used an apparent crack length a* instead of a to take into account geometrical influences to surface defect arising from either coatings filling of crack tip or surface roughness. Notably, the critical tensile stress of fibre with a surface flaw, $\overline{\sigma}_f$, is significantly affected by the coating modulus and thickness. Accordingly, we propose a nondimensional healing efficiency factor, $\varphi = L(1+L/d)E_c/(\beta \cdot a^* \cdot E_f)$ as indication of whether the fibre is sufficiently coated and how the reinforcement effect is

degraded by environmental corrosion. Therefore, the strength improvement ratio, η, can be related to a healing efficiency factor, φ, as

$$\eta = \frac{\sigma_f - \sigma_0}{\sigma_0} = \frac{1}{\sqrt{1-\varphi}} - 1 \qquad (2)$$

where $\sigma_0 = [2 \cdot \gamma \cdot E_f/(\beta \cdot a^*)]^{1/2}$ is the strength of fibre without coatings. More rigorous analysis shows that reducing a* to equilibrium inter-atomic distance, a_0, of atoms at force equal to zero, σ_0 approaches the ultimate theoretical strength of fibre, $\sigma_{max} = E_f/2\pi$. The healing efficiency factor ranges from zero to one representing conditions from non-coating/poor healing case to efficiently healing case. Overall, our glass fibres with nanotube coatings show the highest φ and mechanical strength improvement (Fig. 7).

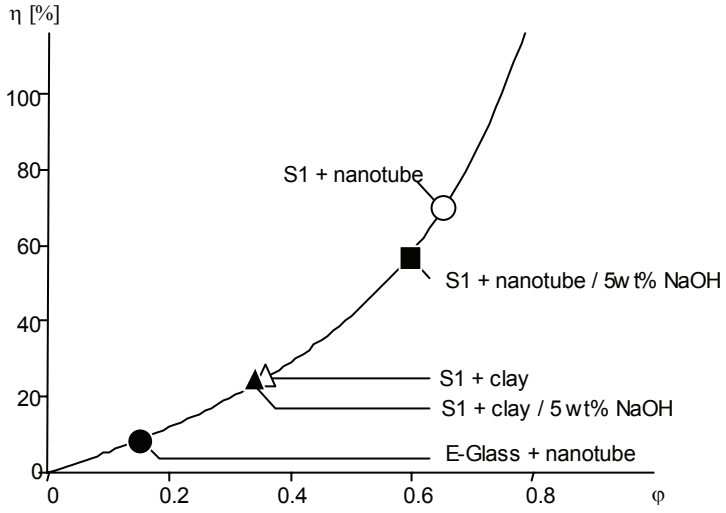

Fig. 7:
Response of strength variation ratio η to healing efficiency factor φ

Generally speaking, the thicker the coating layer and larger the stiffness of coatings the higher are φ and tensile strength of the fibre.

On the other hand, the larger the size of defect and higher the stiffness of fibre, for effective repairing, the thicker and stiffer coatings are required. It implies that the higher strength can be achieved for fibres with surface defects when the healing efficiency factor is closer to one. Moreover, the variation of healing efficiency factor indicates how strong the resistance of the coatings subjected to environmental attack, i.e., no significant reduction of φ for nanoclay coatings after alkaline treatment represents its high environmental barrier and anti-corrosion properties. Finally, the model allows to estimate approximately the coating stiffness based on the tensile strength of fibre. Taking as estimate E_f = 70 GPa, γ = 1.75 J·mol^{-1} for glass [7], and average L = 600 nm for the coatings, we can calculate E_c to be $\approx$ 9 GPa for nanotube coatings and $\approx$ 6 GPa for clay coatings, respectively. These values are reasonably consistent with the calculated theoretical values by rule of mixture (ROM), which are 8 GPa and 3 GPa, respectively, for the two corresponding nanocomposite coatings.

Table 1:
Local interfacial shear strength, τ_d, and critical interfacial energy release rate, G_{ic}, of ARG fibre reinforced cement matrix composite

Fibre	τ_d [Mpa]	G_{ic} [J·mol^{-2}]
Control	23	0.6
Coating C2	25	0.7
S1 + clay	34	2.2
S1 + coating K + clay	57	5.7

To investigate whether the nanocoatings could affect interfacial adhesion, we tested the concrete composites with nanocomposite coated ARG fibres. As compared to the systems without clay (see Table 1), the sized fibre with clay shows a significantly higher local interfacial shear strength τ_d and critical interfacial energy release rate G_{ic}. Interestingly, the sized fibre with additional polymer coating plus clay shows the best performance. The significant increase in adhesion strength is attributed to the mechanical properties and thickness of the hybrid nanocoatings, influencing interface integration and stress concentration. Besides, the coating with clay results in much less degradation due to limited access of the aggressive alkali solution, which consequently increase the frictional component of bond.

Our approach was further extended to single-walled carbon nanotubes (SWCNTs)/E-glass fibre reinforcements and thermoplastic polypropylene filaments using commingled yarn technologies. We utilised a unique melt spinning equipment for E-glass fibre which is compatibly combined with a melt spinning extruder to manufacture commingled yarns. The in-situ commingling allows to combine homogeneously both glass and polypropylene filament arrays in one processing step and without fibre damage compared to commingling by air texturing [8]. Additionally, it permits to apply one sizing formulation to both polymer and glass filaments. We have found that the sizing enables a good strand integrity with the polypropylene yarn. The interfacial adhesion can be improved with a sizing consisting of aminosilane and maleic anhydride grafted polypropylene film former, which results in both improved transverse tensile strength and compression shear strength. The interfacial parameters in GF/PP systems were characterized by single fibre pull-out tests. The data indicates a local adhesion strength of 30.2 MPa to SWNTs compared with 22.1 MPa for the same GF/PP/sizing system without SWCNTs. The critical interface energy release rates determined are 31.8 and 14.0 J·mol^{-2}, correspondingly. The significant improvement of adhesion strength seems to be caused by a different failure mechanism (local interfacial bonding and crack bridging). Due to the mechanical interlinking with SWCNTs the roughness of the fracture surfaces is increased (Fig. 8 a, b) and the phase image (Fig. 8 c) shows material inhomogeneity possibly caused by carbon nanotubes. Overall, the hybrid nanocoatings cause improved fibre strength, corrosion resistance, and interfacial properties. The *in-situ* commingling process technology and nanostructured coatings show promising potential in cost-effective processing of continuous fibre thermoplastic composites for different applications.

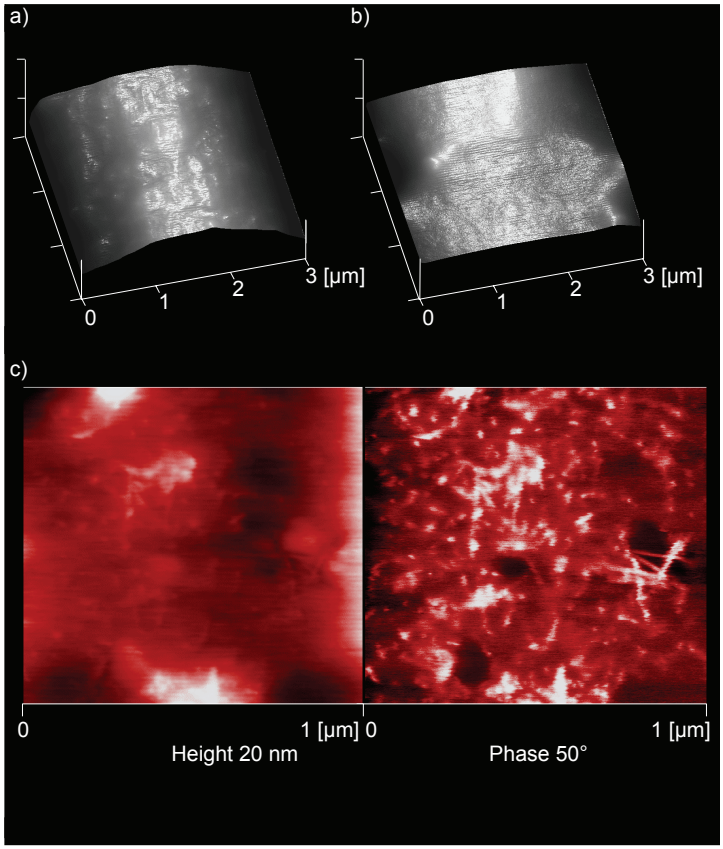

Fig. 8:
AFM topography images of fracture surfaces of a) E-glass fibres without SWCNTs and b) E-glass fibres with SWCNTs in sizing after fibre pull-out test (x, y =3 µm, z = 400 nm). c) AFM topography and phase images, respectively, of E-glass fibres with SWNTs in sizing

References

[1] S.L. Gao, E. Mäder, A. Abdkader, P. Offermann: Langmuir 19 (2003), p. 2496-2506

[2] LM. Ericson, H. Fan, H. Peng, V. A. Davis, W. Zhou, J. Sulpizio, Y. Wang, R. Booker, J. Vavro, C. Guthy, A. Nicholas G. Parra-Vasquez, M. J. Kim, S. Ramesh, R. K. Saini, C. Kittrell, G. Lavin, H. Schmidt, W. Wade Adams, W. E. Billups, M. Pasquali, W.-F. Hwang, R. H. Hauge, J. E. Fischer, R. E. Smalley: Science 305 (2004), p. 1447-1450

[3] M.M. Dubinin: Progress in Surface and Membrane Science.– Vol. 9. New York : Academic Press, 1975

[4] S. Brunauer, P.H. Emmett, E. Teller: J. Amer. Chem. Soc. 60 (1938), p. 309-312

[5] S.L. Gao, E. Mäder, R. Plonka: Acta Materialia 52 (2004), p. 4745-4755

[6] S.L. Gao, E. Mäder, R. Plonka: Acta Materialia 55 (2007), p. 1043-1052

[7] B.R. Lawn: Fracture of Brittle Solids.– 2nd Edition, Cambridge : Cambridge Univ. Press, 1993

[8] E. Mäder, C. Rothe, H. Brünig, T. Leopold: Key Engineering Materials 334 (2006) S. 229-232 in: Adv. Comp. Mat. Struc. Proc. 5th Asian-Australasian Conf. Composite Materials (ACCM-5) / Hrsg. J.K. Kim, D.Z. Wo, L.M. Zhou, H.T. Huang, K.T. Lau, M. Wang, Hong Kong : Trans. Tech. Publications Ltd. (2006)